

# Dynamic Texture Decoding Using a Neuromorphic Multilayer Tactile Sensor

Harrison Nguyen<sup>\*†</sup>, Luke Osborn<sup>\*</sup>, Mark Iskarous<sup>\*</sup>, Christopher Shallal<sup>\*</sup>,  
Christopher Hunt<sup>\*</sup>, Joseph Betthausen<sup>†</sup>, and Nitish Thakor<sup>\*†‡</sup>

<sup>\*</sup>Department of Biomedical Engineering, Johns Hopkins University, Baltimore, Maryland 21218

<sup>†</sup>Department of Electrical and Computer Engineering, Johns Hopkins University, Baltimore, Maryland 21218

<sup>‡</sup>Singapore Institute for Neurotechnology, National University Singapore, 119077 Singapore

Email: hnguye68@jhu.edu

**Abstract**—Prosthetic limbs would benefit from tactile feedback to provide sensory information when interacting with the environment, such as adjusting grasps using force feedback or palpating texture. In this work, we demonstrate how a multilayer tactile sensor can be used for palpation, and enhance the ability to discriminate between touch interfaces. Inspired by mechanoreceptors in skin, the multilayer sensor consists of multiple textile force sensing elements. The novelty of this work lies in the application of a multilayer sensor, one that produces touch receptor like (neuromorphic) output, to texture classification by using a classifier based on sparse recovery. This approach is shown to be capable of palpation, achieving classification accuracies as high as 97% on a distinct texture set. Using compressed sensing and sparse recovery, the multilayer sensor can decode texture under dynamic conditions, potentially providing amputees the ability to perceive rich haptic information while using their prosthesis.

**Index Terms**—Haptics, Tactile Sensor, Neuromorphic Model, Supervised Learning, Compressed Sensing & Sparse Recovery

## I. INTRODUCTION

Amputees face many challenges towards achieving intuitive use of their prosthetic limb [1], [2]. Current state-of-the-art, commercially available prosthetic limbs have complex multi-fingered hand designs and offer basic pattern recognition for control. However, only occasionally basic force feedback is provided to the prosthesis user due to lack of suitable tactile sensor solutions. In recent years, human-machine interfaces such as advanced upper limb prostheses have seen multiple developments in sensor designs for haptic feedback [3], [4]. However, feedback systems that can measure dynamic haptic variables are still under active development. Like human mechanoreceptors [5]–[8], sensors that can measure dynamic haptic variables such as texture and shape could inform how a prosthetic hand should apply active touch, i.e. palpate, when grasping different objects. It is thus important to develop improved solutions for relaying complex tactile information to the prosthesis for robust control of the hand.

Prior work has been done to develop systems that can detect and classify different textures [9]–[12]. In this work, we propose the use of a multilayer tactile sensor design [13] comprised of low cost fabric materials, simple neuron models, and a linear classification algorithm for texture classification. Specifically, we developed a 3x3x2 multilayer sensor to model human mechanoreceptors. A 2 DOF robot was assembled

to apply various textures onto the multilayer sensor. Three textures were designed as a proof of concept to evaluate the sensor's ability to discriminate texture. To compress the information recorded by the multilayer sensor, the output of the sensor was transformed into neuromorphic action potentials or spikes by using 2 Izhikevich neuron models [14] to mimic rapidly adapting (RA) mechanoreceptors and slowly adapting (SA) mechanoreceptors [10], [11] in MATLAB. Using a neuromorphic representation of sensor output has also been shown to improve prosthesis performance for grasping [15] and has even been used to provide sensory feedback [9], so analyzing the output of the multilayer sensor as spikes presents the benefit of both computational efficiency and seamless integration into systems that can send sensory feedback to an amputee. Sparse representation classification (SRC) was chosen to investigate if sparse recovery-based methods, compared to common supervised learning algorithms such as linear discriminant analysis (LDA) or support vector machine (SVM), could use the information recorded by the multilayer sensor to distinguish the 3 textures. Using a low cost and flexibly designed sensor would allow various robotic systems to palpate with their actuators, providing useful contextual information for optimal actuator manipulation.

## II. MATERIALS

### A. Sensor Design

A multilayer tactile sensor was developed to model human mechanoreceptors in skin. A graphic of human skin and actual multilayer sensor can be found in Fig. 1 and Fig. 2. The sensor is based off of an earlier design [13]. Each common line of the multilayer sensor was connected in series with a 100  $\Omega$  resistor in a voltage divider to measure sensor output.

### B. Robot Design

A 2-DOF robot was assembled to apply various loads onto tactile sensors. An Arduino Mega 2560 microcontroller interfaces with a serial electronic scale (7010sb Salter-Brecknell, Fairmont, MN, USA) to measure the force applied to the loading bed. A linear actuator (WindyNation, Ventura, CA, USA) acts along the vertical direction to apply normal loads. The linear actuator was controlled by the microcontroller through an H-Bridge circuit. A proportional control law was

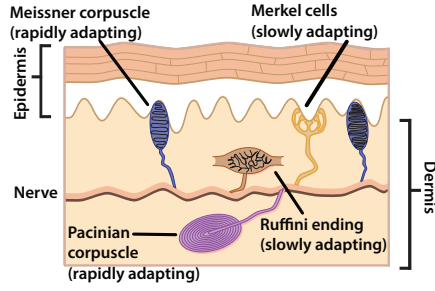


Fig. 1. Graphic depicting the mechanoreceptors found in human skin. Each receptor encodes different haptic features, providing useful feedback information to a person when interacting with the environment via touch.

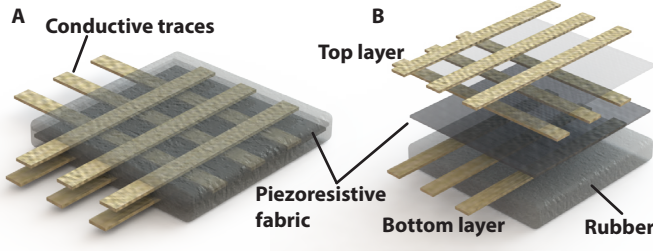


Fig. 2. Overview of the multilayer sensor. (A) The sensing elements are formed by crossing 3 read lines per layer over 3 common lines with a piezoresistive layer in between, leading to 18 sensing elements that have a sensing area of  $3 \times 3 \text{ mm}^2$  and are spaced by 5 mm. (B) The two layers of the sensor, the top layer having more sensitive sensing elements than the bottom layer, reflect how receptors are distributed in different layers of human skin.

used to adjust the actuator's shaft until the scale's output matched a reference force. Simulink was used to determine the value of the proportional gain for the controller based on a model of the system with hardware constraints. The actuator is mounted on a 3D printed cart that is supported by rails. A continuous servo (900-00008 Parallax Inc, Rocklin, CA, USA) slides the cart along a horizontal track to apply tangential loads onto the sensor. Two optical detectors (QRB-1114 Fairchild Semiconductor Corp., Sunnyvale, CA, USA) were used to stop the servo when the cart reached the edges of the track. A diagram of the robot can be found in Fig. 3.

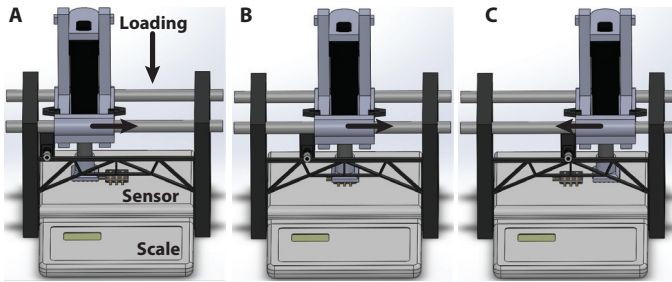


Fig. 3. Graphic depicting operation of the 2 DOF robot for experiments. (A) Once the robot applies a specified load onto the scale, the cart begins to slide. (B) When the cart reaches the center of the track, the robot's probe begins to slide across the multilayer sensor, applying a texture dynamically onto the sensor with the features of the texture running parallel to the sensing elements. (C) Once the cart reaches one end of the track, the cart slides across in the other direction until the other end of the track is reached, where it will repeatedly slide across the sensor for as many trials as desired.

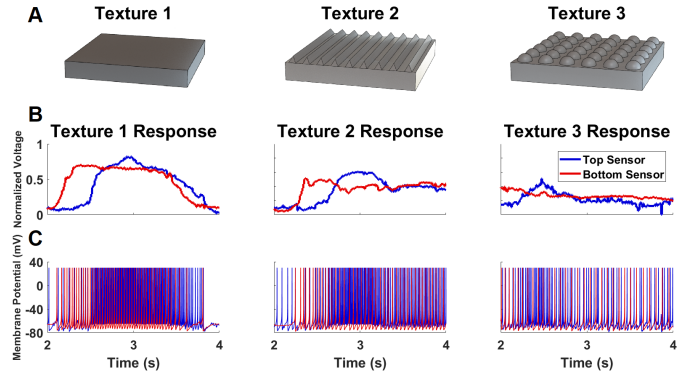


Fig. 4. Overview of the textures and respective example sensing element responses from each layer. (A) One texture was a flat surface. Another texture was a horizontally grated surface with 9 ridges spaced by 2 mm and pitched by a 30-degree draft angle. This texture's grates were applied perpendicularly to the probe's slide. The last texture was a  $6 \times 6$  grid of 4 mm diameter hemispheres spaced by 2 mm edge to edge. (B) Normalized output of sensing elements. (C) Output of the Izhikevich models for each sensing element.

### C. Texture Design

As a proof of concept, 3 textures were developed to observe the sensors response to different textures. Fig. 4A shows the textures used. All textures were placed on a  $36 \times 36 \text{ mm}^2$  square to span the sensor's multiple sensing elements. These texture designs were picked to vary several parameters at once such as pitch, shape, contact area, and size.

## III. METHODS

The main experiment aimed to evaluate the multilayer sensor's ability to palpate different textures. The robot would apply textures onto the sensor using a set dynamic load.

### A. Experimental Procedure

The robot would first use the linear actuator and scale to apply a detectable load of 5 N. The robot would then palpate the textures by sliding its probe over the sensor at a fixed speed of approximately 6.5 cm/s in both directions, pausing for a few seconds at each end of the track to segment each cycle of the robot's trajectory. Several passes across the sensor were performed for each texture as shown in Fig. 3. The microcontroller would sample the sensing element outputs at 100 Hz and record the data in MATLAB during each sliding trial. Over 200 slides were collected for each texture.

### B. Neuromorphic Mechanoreceptor Models

To simulate the behavior of human mechanoreceptors, 2 Izhikevich neuron models [14], regular spiking and fast spiking neurons, are used for the bottom layer and top layer sensing elements respectively based on similar strategies as other works [9]–[12], [16], [17]. Each sensing element was treated as an excitable neuron or receptor that changes voltage in response to a mechanical stimulus. In the Izhikevich neuron model, the artificial neuron's membrane potential  $v$  and recovery variable  $u$  were given by (1) and (2) as follows:

$$\frac{dv}{dt} = 0.04v^2 + 5v + 140 - u + kI \quad (1)$$

$$\frac{du}{dt} = a(bv - u) \quad (2)$$

When the receptor (sensing element) was excited by a stimulus, the input current increased which caused the receptor's membrane potential to depolarize until reaching a threshold, which triggered a spike. The membrane potential then reset to the resting potential and undergoes a refractory period, where the recovery variable was incremented, as shown in (3):

$$\text{if } v \geq 30 \text{ mV, then } \begin{cases} v \leftarrow c \\ u \leftarrow u + d \end{cases} \quad (3)$$

Specifically, the model parameters chosen were  $a = 0.02$ ,  $0.1$ ,  $b = 0.2$ ,  $c = -65$ , and  $d = 8$ ,  $2$  for regular spiking and fast spiking behavior respectively. The normalized sensing element output voltages serve as input currents into the neuron models and were scaled by a gain factor  $k$  such that the maximum spiking rate was 100 spikes/second for SA receptor behavior and 200 spikes/second for RA receptor behavior [7], [8]. Sample sensor responses and the corresponding spiking outputs from the models can be found in Fig. 4B-C.

Once the experiment for the sensor was complete, all of the sensor's responses to each texture were converted into spikes offline by implementing the neuron models in MATLAB. The sensor data collected was segmented in 5 s windows and, since the Izhikevich model was implemented on the scale of milliseconds, underwent a zero-order hold for 10 ms to capture the dynamics of each sliding trial on a millisecond scale. Once the output of each sensing element was transformed into a neuromorphic representation, the mean spike rate and average interspike interval were computed to compress the information from the generated spikes of each trial into a feature vector. Spike rate was computed by counting the number of spikes within a bin of 100 ms and dividing the total by the bin length, leading to 50 spike rates per data window in which the nonzero spike rates are averaged for a mean spike rate. Interspike interval (ISI) was defined as the average time elapsed, in milliseconds, between each spike in a window.

### C. Classification Algorithms

Using multiple trials of the multilayer sensor's response to each texture, we can use key features from the sensing elements as inputs for classification. For each trial, one sample is obtained by concatenating the mean spike rate and average ISI from each of the sensing elements into a single vector  $\mathbf{y} \in \mathbb{R}^{18}$  per layer. Each of these samples can then be used as training data for a classifier or as an input test measurement for classification. To verify the utility of the multilayer sensor, the sensing element outputs from the top layer, bottom layer, and both layers, leading to  $\mathbf{y} \in \mathbb{R}^{36}$  using all sensing elements, of the multilayer sensor are used to train and test the classification algorithms in 3 separate classification tasks.

Since the textures are accessible, we can use supervised learning algorithms for texture classification. Supervised learning algorithms such as LDA and SVM can be used for this classification task since the features of data for each of these classes suggest high separability between classes, such

algorithms typically use a linear kernel, and are relatively simple and efficient to implement. LDA was chosen based on the observed consistency, with slight variance, of the sensor's response to each texture and SVM was chosen based on the observed distinctness of the responses to each texture. LDA and SVM were implemented using the MATLAB Statistics and Machine Learning Toolbox. While these classifiers are commonly used, their performance relies on a training set which may not capture some possible variants of the data. Thus, we are interested in evaluating the use of robust classification algorithms based on compressed sensing such as SRC.

SRC presents a robust strategy, based on prior success in face recognition and EMG pattern recognition [18]–[20], of representing a new multilayer sensor response as a linear combination of a sparse set of sample training responses regardless of signal corruption or variation. In SRC, the training samples from each texture form a subdictionary  $\mathbf{A}_i$  which are concatenated into a full training dictionary i.e.  $\mathbf{A}_{train} = [\mathbf{A}_1 \ \mathbf{A}_2 \ \mathbf{A}_3]$ . Once the training samples of  $\mathbf{A}_{train}$  are normalized, a test sample  $\mathbf{y}$  is to be reconstructed as a weighted linear combination of a sparse number of training samples  $\mathbf{y} = \mathbf{A}_{train}\mathbf{x}$ . To recover the training sample weights  $\mathbf{x}$ , we can solve the following  $l^0$ -minimization problem:

$$\mathbf{x}_0 = \underset{\mathbf{x}}{\operatorname{argmin}} \|\mathbf{A}_{train}\mathbf{x} - \mathbf{y}\|_2 \text{ s.t. } \|\mathbf{x}\|_0 \leq \mathcal{S} \quad (4)$$

The sparsity constraint  $\mathcal{S}$  (set to  $\mathcal{S} = 5$  empirically) ensures the sparsity of  $\mathbf{x}$  by penalizing samples that encode noise in  $\mathbf{y}$ . We solve (4) by implementing Orthogonal Matching Pursuit (OMP), a greedy pursuit algorithm that iteratively searches the training dictionary to find a sparse, approximately orthogonal set of training samples that best represent a test sample [21]. Once the code  $\mathbf{x}$  is recovered, we can identify which training samples from each of the textures were selected to represent  $\mathbf{y}$  since  $\mathbf{x} = [\mathbf{x}_1 \ \mathbf{x}_2 \ \mathbf{x}_3]^T$ , where each  $\mathbf{x}_i$  belongs to a texture. A class  $\hat{c}$  is assigned to  $\mathbf{y}$  by finding the class that solves  $\hat{c} = \underset{i}{\operatorname{argmin}} \|\mathbf{y} - \mathbf{A}_i\mathbf{x}_i\|_2$ ,  $i = 1, 2, 3$  i.e. pick the texture class that has the smallest reconstruction residual.

Since the sensor's response was observed to be mostly consistent and distinct between the 3 unique textures, all classifiers used only 10 randomly selected samples of each texture for the training set and 200 samples of each texture were used as testing samples. This process was repeated 1000 times to reduce the bias of each randomly chosen training sample on the training set.

## IV. RESULTS & DISCUSSION

The classification results, as seen in Fig. 5, showed that compact information from a neuromorphic representation of the sensor's output can be used to reliably discriminate between the three textures through the chosen classifiers. Notably, all classifiers provided reliable classification even though a few number of observations (10) from each texture were used as training data compared to the dimensionality, 18 features for a single layer or 36 features for the full multilayer, of the sensor's outputs. This is consistent with the observation

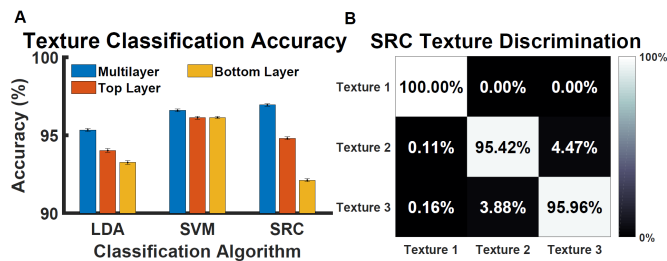


Fig. 5. Texture classification results. (A) Classification results based on different sets of layers. The multilayer sensor reliably distinguishes the textures, with LDA achieving 95.3% accuracy, SVM achieving 96.6% accuracy, and SRC achieving 97% accuracy. Standard error of the average classification accuracy is represented by the error bars. (B) The SRC algorithm's accuracy. The sensor can best distinguish between flat (texture 1) and nonflat textures.

that the sensor has a distinct and repeatable response to each texture. As seen in Fig. 5A, all classifiers using both layers provide more accurate discrimination than using either the top layer or bottom layer alone for classification. While a single layer sensor can achieve decent texture classification ( $>90\%$  accuracy), we hypothesize that by including both layers and achieving better classification that the multilayer sensor will likely be able to discriminate more dynamic touch interfaces than a single layer sensor. For algorithm performance, SRC and SVM achieve better results than LDA for most classification tasks. At 97% accuracy, SRC's performance shows promise for robust classification of the sensor's response to different textures regardless of signal corruption or variation.

## V. CONCLUSION

We showed how a multilayer tactile sensor can be used to palpate texture. The multilayer sensor provided sufficient information via a neuromorphic representation to classify the different textures with high accuracy. The sensor's experiment serves as a proof of concept investigation for exploring the discriminability of different parameters of texture such as spacing and pitch and the decoding of other haptic features such as curvature. With a reliable system for palpation, robotic systems such as prosthetic limbs could use the multilayer sensor for dexterous manipulation of objects or the environment. Potentially, sensory feedback, such as through peripheral nerve stimulation, could use the haptic information detected by the multilayer sensor to elicit percepts of haptic phenomena such as texture or shape [9], [17], [22]. By restoring the perception of rich haptic information, amputees can seamlessly use their prosthetic limb and come closer to viewing their limb as their own rather than as an external device.

## ACKNOWLEDGMENT

This project was partially funded by Johns Hopkins Space Consortium through the Space@Hopkins funding initiative. The SRC and OMP algorithms are primarily based off of lectures from "Compressed Sensing and Sparse Recovery" at Johns Hopkins University taught by Dr. Trac Duy Tran.

## REFERENCES

- [1] E. Biddiss and T. Chau, "Upper-limb prosthetics: critical factors in device abandonment," *Am. J. Phys. Med. Rehabil.*, 2007, vol. 86, pp. 977-987.
- [2] A. E. Schultz, S. P. Baade and T. A. Kuiken, "Expert opinions on success factors for upper-limb prostheses," *J. Rehabil. Res. Dev.*, 2007, vol. 44, pp. 483-489.
- [3] A. F. Russell, R. S. Armiger, R. J. Vogelstein, S. J. Bensmaia and R. Etienne-Cummings, "Real-time implementation of biofidelic SA1 model for tactile feedback," *Conf. IEEE Eng. Med. Biol.*, 2009, pp. 185-188.
- [4] L. Osborn, R. R. Kaliki, A. B. Soares and N. V. Thakor, "Neuromimetic Event-Based Detection for Closed-Loop Tactile Feedback Control of Upper Limb Prostheses," *IEEE Trans. Haptics*, 2016, vol. 9, no. 2, pp. 196-206.
- [5] K.O. Johnson, "The roles and functions of cutaneous mechanoreceptors," *Curr. Opin. Neurobiol.*, 2001, pp. 455-461.
- [6] Y. Roudaut, A. Lonigro, B. Coste, J. Hao, P. Delmas, M. Crest, "Touch sense: Functional organization and molecular determinants of mechanosensitive receptors," *Channels*, 2012, 6(4), pp. 234-245.
- [7] M. Knibestöl, "Stimulus-response functions of rapidly adapting mechanoreceptors in the human glabrous skin area," *J. Physiol.*, 1973; 232(3): 427-452.
- [8] H. Haerle, E.A. Lumpkin. "Merkel Cells in Somatosensation," *Chemosens. Percept.*, 2008,1(2), pp. 110-118.
- [9] C. M. Oddo *et al.*, "Intraneural stimulation elicits discrimination of textural features by artificial fingertip in intact and amputee humans," *eLife* 5, e09148 (2016).
- [10] M. Rasouli, Y. Chen, A. Basu, S. L. Kukreja and N. V. Thakor, "An Extreme Learning Machine-Based Neuromorphic Tactile Sensing System for Texture Recognition," *IEEE Trans. Biomed. Circuits Syst.*, vol. 12, no. 2, pp. 313-325, 2018.
- [11] U. B. Rongala, A. Mazzoni, and C. M. Oddo, "Neuromorphic artificial touch for categorization of naturalistic textures," *IEEE Trans. Neural Netw. Learn. Syst.*, pp. 126130, 2015.
- [12] K. E. Friedl, A. R. Voelker, A. Peer, and C. Eliasmith, "Human-inspired neurobotic system for classifying surface textures by touch," *IEEE Robot. Autom. Lett.*, vol. 1, no. 1, pp. 516-523, Jan 2016.
- [13] L. Osborn, H. Nguyen, J. Betthausen, R. Kaliki and N. Thakor, "Biologically inspired multi-layered synthetic skin for tactile feedback in prosthetic limbs," *Conf. IEEE Eng. Med. Biol.*, 2016, pp. 4622-4625.
- [14] E. M. Izhikevich, "Simple model of spiking neurons," *IEEE Trans. Neural Netw.*, vol. 14, no. 6, pp. 1569-1572, Nov. 2003.
- [15] L. Osborn, H. Nguyen, R. Kaliki and N. Thakor, "Prosthesis grip force modulation using neuromorphic tactile sensing," *Proc. Myoelec. Controls Symp.*, 2017, 188-191.
- [16] A. Sahasranamam, I. Vlachos, A. Aertsen, A. Kumar, "Dynamical state of the network determines the efficacy of single neuron properties in shaping the network activity," *Sci. Rep.*, 2016; 6: 26029.
- [17] L. E. Osborn, A. Dragomir, J. L. Betthausen, C. L. Hunt, H. H. Nguyen, R. R. Kaliki, N. V. Thakor, "Prosthesis with neuromorphic multilayered e-dermis perceives touch and pain," *Sci. Robot.* 3, eaat3818, 2018.
- [18] J. Wright, A. Y. Yang, A. Ganesh, S. S. Sastry and Y. Ma, "Robust Face Recognition via Sparse Representation," *IEEE Trans. Pattern Anal. Mach. Intell.*, vol. 31, no. 2, pp. 210-227, Feb. 2009.
- [19] J. L. Betthausen, L. E. Osborn, R. R. Kaliki and N. V. Thakor, "Electrode-shift tolerant myoelectric movement-pattern classification using extreme learning for adaptive sparse representations," *Conf. IEEE Biomed. Circuits Syst.*, 2017, pp. 1-4.
- [20] J. L. Betthausen, C. L. Hunt, L. E. Osborn, M. R. Masters, G. Levay, R.R. Kaliki and N. V. Thakor, "Limb Position Tolerant Pattern Recognition for Myoelectric Prosthesis Control with Adaptive Sparse Representations From Extreme Learning," *IEEE Trans. Biomed. Eng.*, vol. 65, no. 4, pp. 770-778, April 2018.
- [21] J. A. Tropp and A. C. Gilbert, "Signal Recovery From Random Measurements Via Orthogonal Matching Pursuit," *IEEE Trans. Inf. Theory*, vol. 53, no. 12, pp. 4655-4666, Dec. 2007.
- [22] L. Osborn, M. Fifer, C. Moran, J. Betthausen, R. Armiger, R. Kaliki and N. Thakor, "Targeted transcutaneous electrical nerve stimulation for phantom limb sensory feedback," *Conf. IEEE Biomed. Circuits Syst.*, 2017, pp. 1-4.